ISTITUTO NAZIONALE DI FISICA NUCLEARE

Sezione di Milano

INFN/AE-93/26
1 Dicembre 1993

G. Battistoni:

MONTE CARLO SIMULATIONS IN HIGH ENERGY COSMIC RAY PHYSICS

PACS.: 96.40.Tv; 96.40.De; 98.70.Sa

Servizio Documentazione
dei Laboratori Nazionali di Frascati

INFN - Istituto Nazionale di Fisica Nucleare
Sezione di Milano

INFN/AE-93/26
1 Dicembre 1993

MONTE CARLO SIMULATIONS IN HIGH ENERGY COSMIC RAY PHYSICS

G. Battistoni
INFN, Sezione di Milano, via Celoria 16, I-20133 Milano, Italy

Presented at the IV Int. Conf. on Calorimetry in High Energy Physics,
La Biodola (Is. d'Elba), Italy, Sept. 20-25 1993

Abstract

A few aspects of the simulation strategies as required in present high energy cosmic ray physics are briefly reviewed. The analysis of deep underground muons and of the e.m. component of Extensive Atmospheric Showers are considered as examples. The possible use of standard codes adopted in accelerator physics is also discussed.

1. Introduction

At present an intense activity exists in the field of high energy cosmic ray physics. The main goal is to understand the origin, acceleration, and propagation mechanisms of these high energy particles and nuclei. These are distributed over an extremely wide energy spectrum (up to 10^{20} eV events have been observed), falling approximately as a power law $\sim E^{-\gamma}$. A steepening of the spectral index γ from $\sim$2.7 to $\sim$3.0 is observed around 10^{15} eV ("knee" of the spectrum). The understanding of the origin of such a knee is considered as one of the fundamental issues. In particular, it is of great importance to reach definitive conclusions about the mass composition of primary cosmic rays around and above the knee, i.e. the relative fraction of protons with respect to heavier nuclei. For a basic review on the argument see ref. [1]. At present controversial measurements exist. While at energies below a few tens of TeV direct measurements are possible by means of stratospheric balloons or space stations, at higher energy this is no more feasible: as an order of magnitude, the number of primaries with energy exceeding 10^{15} eV is $\sim$ 70 $m^{-2} \cdot sr^{-1} \cdot year^{-1}$. Therefore only indirect measurements are possible in this range, i.e. through the properties of secondary particles produced by the interaction of primaries with the atmosphere (Extensive Air Showers). It is evident how the interpretation of these results has to rely necessarily upon simulation. This is a task which, due to the scale of relevant quantities, requires an effort comparable or greater with respect to similar activities in accelerator physics. The particular nature of the problem usually asks for short-cuts or "ad hoc" simulation strategies. A brief discussion on these strategies, far from being exhaustive, is presented in section 2. A crucial role is played by the hadronic interaction model, whose problematics is summarised in section 3. As typical examples of simulation application the analysis of deep underground muons and of the e.m. component of Extensive Air Showers are presented in section 4 and 5 respectively.

The short discussion presented here does not include many important aspects of the research in high energy cosmic ray physics. Among the missing items of particular interest are the simulation problems for underground or underwater high energy neutrino detectors.

2. Simulation Strategies

A first technical complexity, as compared to accelerator experiments, comes from the fact that in cosmic ray problems there is not, usually, a point-like interaction region, but a wide solid angle source has to be considered. In the high energy region, primary cosmic rays have an isotropic angular distribution, deviations being at the 10^{-3} level. Typical angular coordinates are the zenith (measured from the vertical), and the azimuth (measured clockwise from North). Impact position of primary direction has to be uniformly sampled over an area, orthogonal to the considered arrival direction, sufficiently larger than the detector itself, since a trigger may occur from part of a shower whose core can be far off the apparatus. The extension of such a sampling area clearly depends on the particular conditions of a given experiment; examples of relevant parameters are the transverse structure of the shower, the size and the site of the detector, the energy region considered, etc. The energy sampling deserves some care, since several decades of energies, over a power-law falling spectrum usually contribute to the data sample of an experiment. In order to avoid fluctuation problems the energy interval can be subdivided in bands and the partial results are eventually summed up. The minimum energy is dic-

tated by threshold considerations, while the maximum depends on the experimental time interval under analysis. The energy limits, the exposure time, the sampling area, and the angular window fix the number of primary particles to be generated at simulation level, for a given energy spectrum and composition model. The total number may be extremely high, and the dominant factor is in general the energy threshold, due to the spectrum shape. Therefore the primary achievement in simulation is to reach enough speed and simplification without appreciable loss in the results. A first handle is of course the energy cut of secondary particles. In the case of experiments measuring only deep underground muons, for instance, the minimum energy for a muon to reach the detectors is determined by the rock overburden: this allows automatically the use of high energy cuts (hundreds of GeV, typically), thus discarding also the abundant electron/photon component. However, this is not the case when the surface e.m. component is needed, in EAS arrays, or in the simultaneous measurement of surface e.m. size and deep underground muons (see ref. [2]). Here an energy cut down to the MeV level, or below, is requested. Biasing techniques are often of little use, since correlation of measurable quantities in the same event may be important. A typical example is the N_e–N_μ correlation. Not only are average values requested, fluctuations play a fundamental role. This can be easily understood, for instance, in the case of a surface EAS array: as compared to a calorimeter, such an array performs, for each event, a single sampling of a shower at a given depth. A large use of analytical formulas (solutions of the shower transport equations under different approximations) has been made, as far as the e.m. size is concerned. This point will be re-examined in section 5.

The use of parameterizations is one of the most frequent solutions to speed up calculations. An example of parameterization of Monte Carlo results for underground muons (NIM85[3]) was presented with the explicit aim of providing the tools to build fast generators. This turns out to be a successful strategy in some cases, however once again the correlation between different parameterized quantities is lost. Oversampling of the events is also a trick which can be used in some cases (take for instance the operation of sampling the impact point). Here the danger of introducing unwanted under fluctuations must be considered.

There are experiments which, near the extreme end of the spectrum, measure the position of maximum in the shower, or the rate of change of shower maximum as a function of LogE ("Elongation rate"). The most famous example is the Fly's Eye[4]. Here the generation of the transverse structure of the interaction, and of the shower, is obviously very simplified.

A useful strategy for an experiment is the use of shower banks. For example, in order to avoid different generations for different test composition models, different mass groups (usually five are enough: H,He,CNO,Si,Fe) can be generated with a properly chosen energy spectrum $\Phi_1(E)$. Any test composition model can be constructed by sampling the events from the different mass banks, with a weighting (or rejection) factor which, at each energy E_0, is just the ratio $\Phi^j(E_0)/\Phi_1(E_0)$; $\Phi^j(E)$ is the differential energy spectrum of the desired model for the j-th mass group.

A brief discussion on particle transport in the atmosphere is also of some interest. Due to the homogeneous material, the shower simulation in the atmosphere can offer some technical advantages with respect, for instance, to the case of a shower in a sampling calorimeter. The absence of abrupt discontinuities in the material and in the geometrical set-up, allow a relevant saving of computer time. The very long extensions (tens of km)

and the non constant density are only apparent problems. In the specialised codes, transport routines are explicitly designed to work in gr/cm^2 units and whenever a conversion to metrical units is necessary, the use is made of analytical relations describing the vertical profile of the "standard atmosphere" (Shibata fit, see ref. [1]). As an example, in Fig. 1 the height-depth relation, between 2 and 36 km a.s.l., is shown. In this way the set-up can be treated as an infinitely extended medium. Care must be taken if zenith angles exceeding 60° are needed, since the earth curvature is then no more negligible.

3. The Hadronic Interaction Model

The hadronic interaction model plays a significative role in the simulation chain. In practice most of present codes operate in the context of superposition model, where a projectile nucleus of mass number A and total energy E_0 is treated as A independent nucleons with energy E_0/A. This is considered a reasonable approximation, however there should exist some correlation effects. The problem is thus reduced to that of nucleus-nucleus collisions with the inclusion of nuclear target effects. Up to 1000÷ 2000 TeV/nucleon the c.m. energy is still within the energy range of existing colliders. Therefore, the inelastic σ_{p-Air} and σ_{N-Air} cross sections can be reliably obtained through the Glauber model, starting from the existing data on σ_{p-p}. Secondary meson production is described by the inclusive cross sections

$$E\frac{d^3\sigma_{p\pi,pK}}{dp^3} \tag{1}$$

These ones instead are poorly known in the kinematical region of interest, which is the fragmentation region. It is usually assumed that only mild Feynman scaling violations occur in the very forward region; it has been demonstrated how the rate of uncorrelated high energy muons is dominated by the decay of mesons produced at high x_F; they are proportional to the "Z" function[5], which in the case of charged pions is defined as follows:

$$Z_{p\pi^\pm} = \int_0^1 x^\gamma \frac{dN_{p,\pi^\pm}}{dx} dx \tag{2}$$

where dN/dx is distribution of charged pions produced in proton collisions with nuclei in the atmosphere, and γ is here the integral spectral index (~ 1.7). The value of γ is such that the high x values (where measurements are generally poor) have a dominant weight. Usually, extrapolations from existing data are needed to build a model.

The transverse structure of the shower is related to the P_t distribution of secondary mesons. The knowledge of this is essential in order to reproduce the acceptance of a finite size detector. Due to the wide range of energy requested, the correct evolution of P_t with energy is essential. Again the P_t behaviour at high x_F is not well known and one has to rely upon some modelization. Moreover the effect of nuclear target, such as the so called Cronin effect[6], has to be treated correctly.

As far as heavy flavours production is concerned, in general their contribution can be neglected. This is not the case for particular measurements, such as the analysis of the prompt (isotropic) high energy muon component.

Among global parameters, the inelasticity, usually defined as the fraction of energy not carried away by the leading baryon, has some importance since it is related to the longitudinal development of the shower. The amount of diffractive scattering also enters

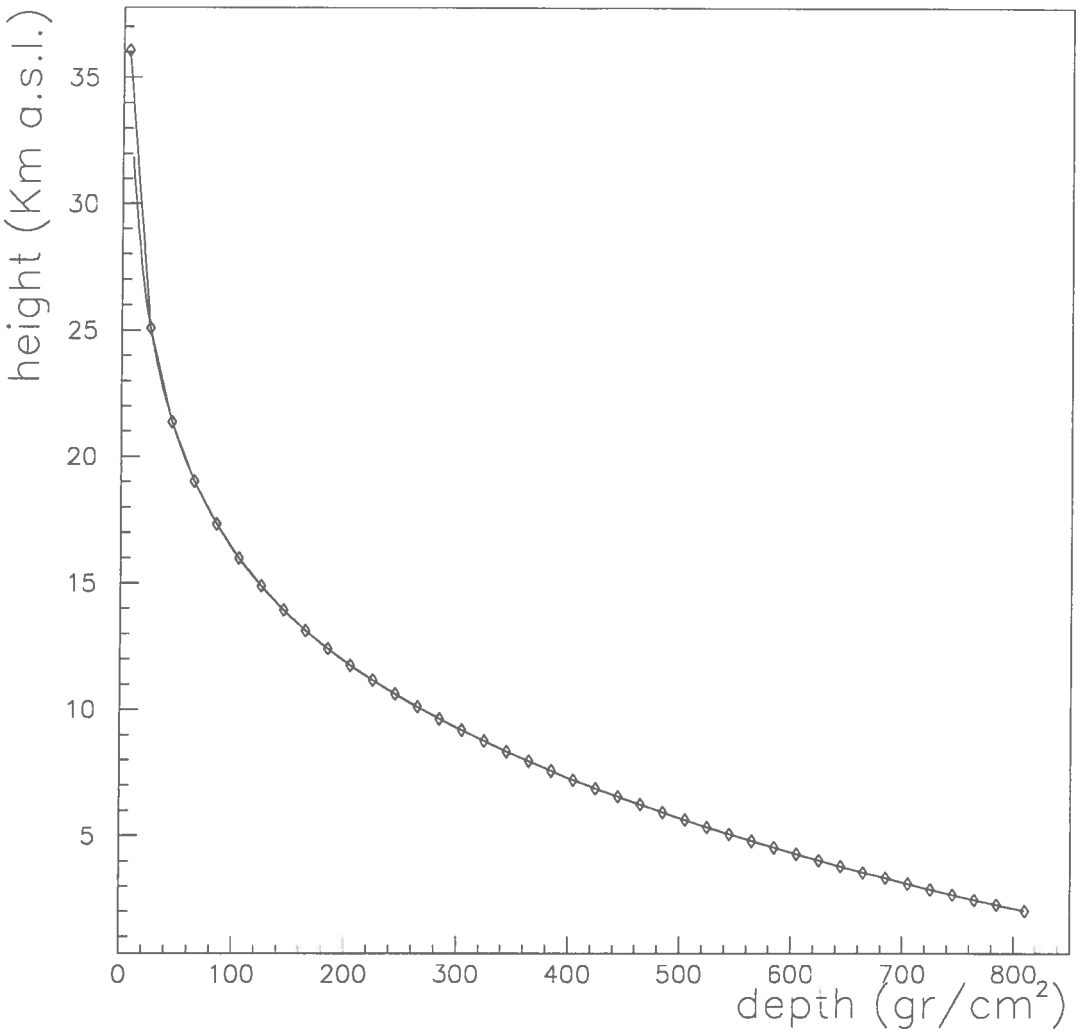

Figure 1. The profile of the standard atmosphere used in the simulation setup for atmospheric showers. The marked points are separated by 0.5 X_0. The solid line is a piece-wise linear approximation

in determining the average inelasticity. Experiments sensitive to the position of shower maximum seem to prefer high inelasticity models[4].

At present a number of hadronic interaction codes exist for high energy physics, but often they are designed for accelerator experiments, running at fixed energy, and in general they are tailored for the particle production in the central region. For technical reasons it is extremely difficult to include them in a shower program. Specialised codes and algorithms have been constructed for cosmic ray applications. A fast splitting algorithm with pure scaling, based on energy conservation, was developed by Hillas[7] and it was at the basis of aforementioned NIM85 code for underground muons[3]. Another attempt is the HEMAS code[8], which is based on the parameterization of minimum bias events at SpS by the UA5 experiment[9], generalised to nuclear targets. Multiplicity and pseudorapidity distributions reproduce collider data in the central region up to $\sqrt{s} \leq 900$ GeV. Projectile diffraction is included. The results of such a code were again parameterized to provide a fast generator for underground muon physics. HEMAS is embedded in a shower program which allows to follow the shower development in the atmosphere with an energy cut on secondary particles down to 0.5 TeV. It also includes a three-dimensional muon propagation code in the rock. A different approach is the SIBYLL code[10], where an attempt has been done in order to derive the detailed features of the interaction from an underlying physical model. This is the Dual Parton Model[11], with the inclusion of mini-jet production, preserving unitarity. Diffraction is also considered here. In ref. [12] a comparison of the mentioned models, together with other ones, is presented, as far as high energy muon production is concerned. It is surprising how models, which are constructed from extremely different approaches, give in fact results not far one from the other, as far as a few quantities like $< N_\mu(E \geq 1\ TeV) >$ are concerned. As an example, in fig. 2 it is shown the comparison of the distribution of underground muons (zeros included), at the depth of 3400 m w.e. (a), and of e.m. size at 2000 m a.s.l. (b), for 1000 TeV protons at 33.5° of zenith, as produced using HEMAS and SIBYLL, for the same shower program and muon transport. The average N_μ varies by ~10% , while the average $LogN_e$ is practically unchanged. More important differences appear in the $< P_t >$ from the different models.

In order to overcome some drawbacks of the superposition scheme, the fluctuations of the interaction lengths of nuclear projectiles in the atmosphere should be considered. A realistic mode for cosmic ray application is provided by the NUCLIB code[13].

4. The Analysis of Underground Muons

As an example of simulation for an experiment exploring the 1000 TeV region, the recent analysis of multiple muon events underground as performed by the MACRO[14] experiment, at the Gran Sasso Laboratory, is summarised here. Deep underground (≥3100 m w.e.) the MACRO experiment is able to track the penetrating high energy muons ($E_\mu \geq 1.3$ TeV in the atmosphere) over a large projected area (~ 900 m^2). The analysis of the muon flux in the detector as a function of event multiplicity is performed by comparing the experimental results to the prediction coming from external input models of spectrum and composition.

The large area of MACRO detector allows the study of muon separation with negligible detector bias. Such a distribution function is largely determined by the hadronic interaction properties: the P_t distribution of secondary mesons and inelastic cross sec-

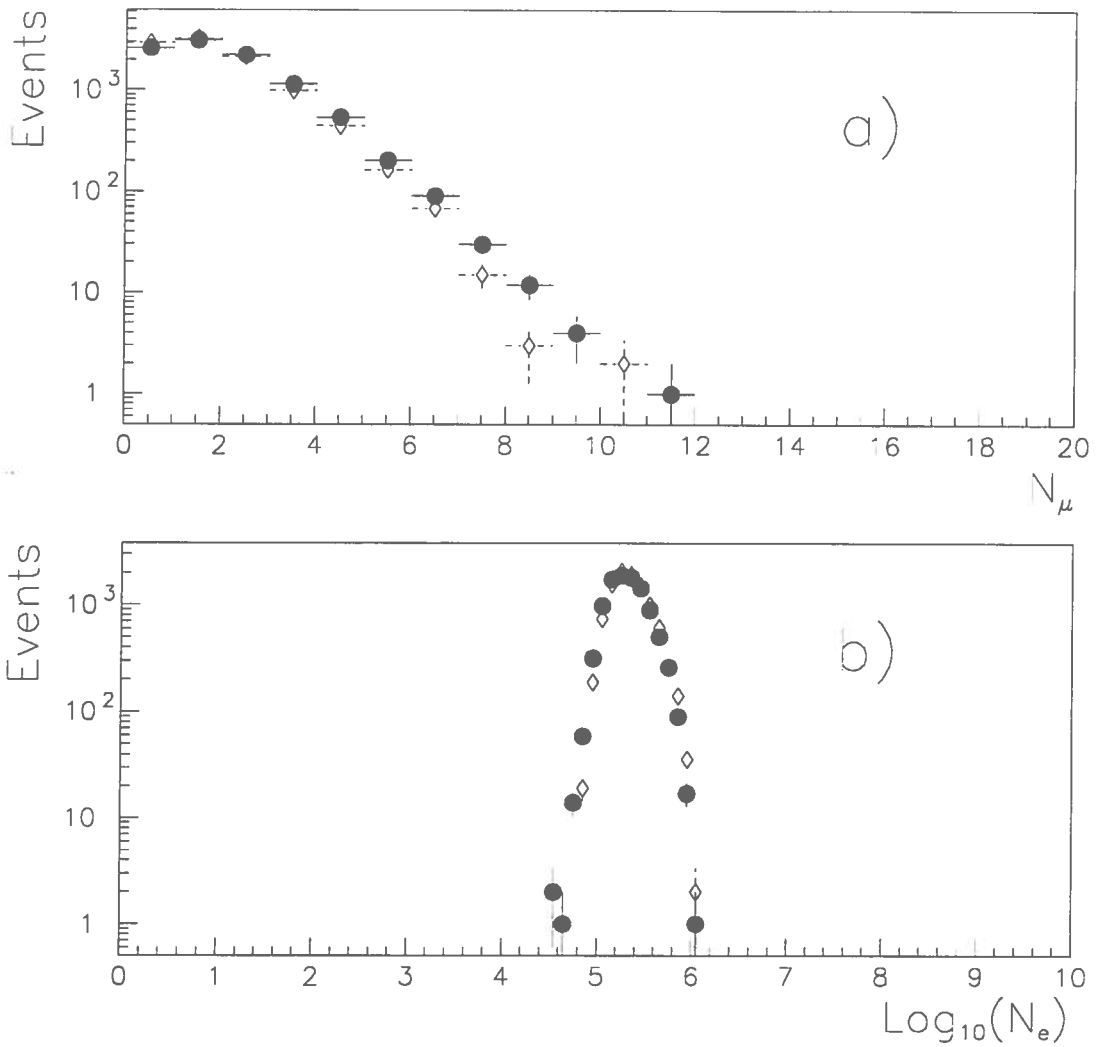

Figure 2. Distribution of underground muons (zeros included), at the depth of 3400 m w.e. (a), and of e.m. size at 2000 m a.s.l. (b), for 1000 TeV protons at 33.5° of zenith, as produced using HEMAS (black symbols), and SIBYLL (open symbols).

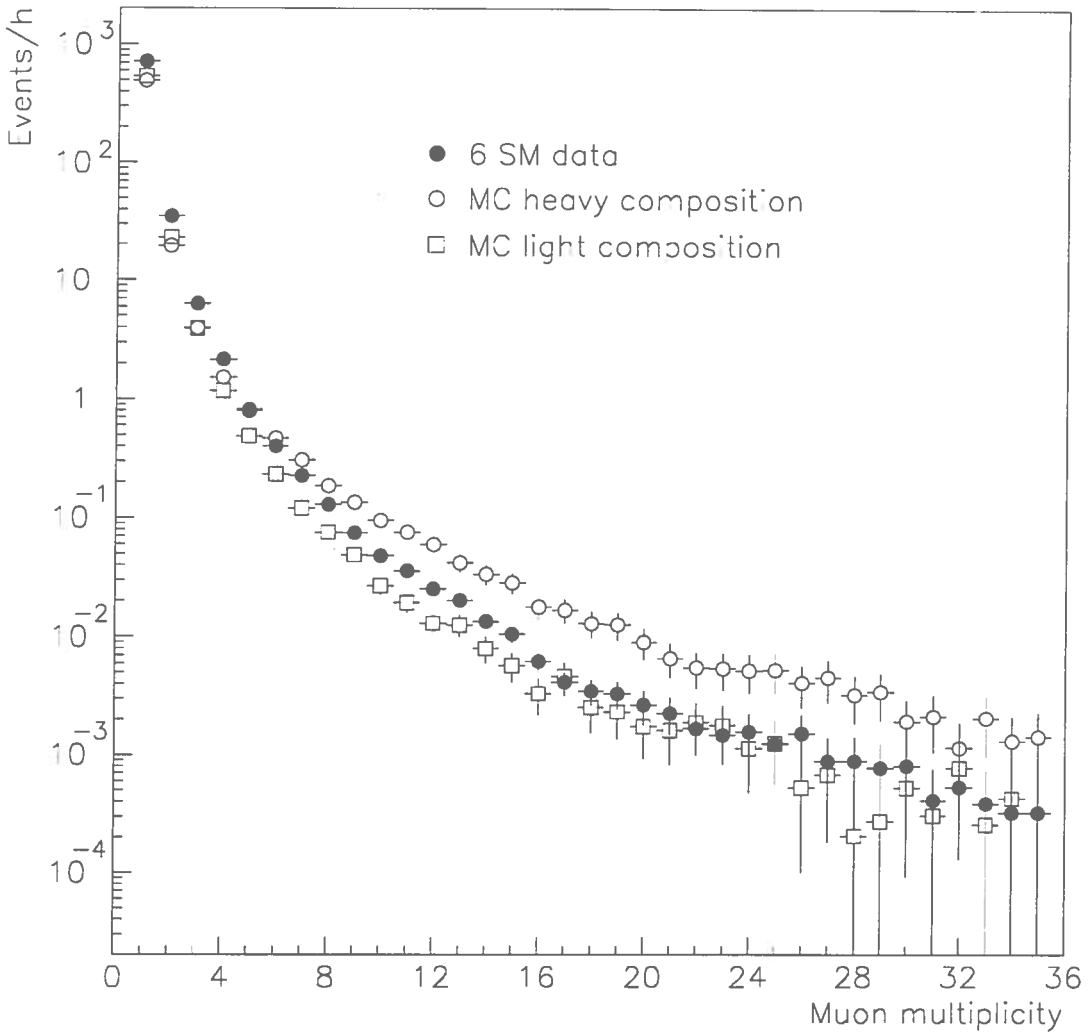

Figure 4. Rate distribution of event multiplicity detected in MACRO compared to simulation results with two extreme composition models

concerning muons with energy in the TeV region or above, where the bremsstrahlung process dominates the fluctuations in energy loss. By means of the FLUKA transport code[26] the intensity of muons as a function of depth in standard rock (assuming the atmospheric muon spectrum suggested in ref. [1]) has been calculated[27], with both the old[21] and new[25] formula for bremsstrahlung. The result for the depth-intensity curve is shown in fig. 5. Similar results where obtained in ref. [28]. The difference is relevant at very large depths, however, already at the depth of MACRO a 5% factor in the total rate of simulated events could be attributed to such an uncertainty. The same process would bring, according to a preliminary evaluation, to a 10% uncertainty on the calculated $< N_\mu >$. It is astonishing how the uncertainty in muon transport gives a systematic error comparable to that coming from the uncertainty in the interaction model. However, we have also to consider that most of formulations for muon energy loss do not include radiative corrections[22]; their inclusion might appreciably change the quoted results.

5. The e.m. Shower in Atmosphere

The accurate simulation of large statistic of EAS produced by a primary nuclei ranging up to 10^5 TeV and beyond is a formidable task in terms of computing power. Cosmic ray shower generators provide the opportunity to follow tridimensionally the secondary particles produced at different depth in the atmosphere (e.g. photons from π^0 decay, electrons from semileptonic decays of K, etc.) In order to maintain computer time within reasonable limits, these secondaries are followed up to a relatively high energy threshold. It is then assumed that each of these secondary can give origin to a sub-shower contributing to the total e.m. "size" measured by air shower arrays. The average number of electrons/positrons arriving at the depth of the shower array from each sub-shower is usually derived from analytical shower approximations already existing in the literature. Fluctuations of individual sub-showers are neglected since they are overwhelmed by the fluctuations in the development of the Extensive Air Shower itself. The use of such analytical approximations is known to introduce systematic errors, so that new attempts are under way. The general trend is to try to make use of the results of specialised shower programs commonly used in high energy physics (GEANT[29], EGS4[30], FLUKA[26], etc.). One possibility is to create, at some level, an interface between a specialised cosmic ray code and one of the mentioned shower codes. Otherwise, an attempt has been made to create a pre-recorded set of showers[31] which is addressed by an EAS general simulation. In this case the limitation is given by the size of the requested dynamical memory. Here I describe another approach[32], in which a set of parameterizations of Monte Carlo results is obtained in order to describe the sub-showers initiated by secondary particles at different energies at different depth in the atmosphere. These parameterizations are given for the number of particles, the lateral distribution, and the energy distribution of the electromagnetic component of EAS induced by gamma-initiated sub-showers in the energy range $10 \div 10^5$ GeV, and by electron-initiated sub-showers in the energy range $10 \div 10^4$ GeV, at different detector depths (X_{det}) and for starting points in the atmosphere (X_{start}) ranging between $10 \div 1000$ gr/cm^2. The motivation to limit the energy range of electron-initiated sub-showers with respect to the case of gamma-initiated ones comes from an analysis of the energy distribution of secondary particles in EAS according to the HEMAS simulation. The features of the electromagnetic cascade allow to express the results in term of the total thickness expressed in radiation length, independently

tions which are related to the production heights. At the same time the dependence of the muon decoherence function on the primary composition is small. Therefore, such an experimental study gives the opportunity to test some fundamental feature of an interaction model. On the other hand, the knowledge of the muon separation distribution is essential in the analysis of muon multiplicity inside the detector, since it determines the fraction of muons in a bundle which enter the detector acceptance. A detector independent analysis performed by MACRO[15] has shown how the experimental data are reasonably described by the interaction model contained in the HEMAS code[8], rejecting completely the NIM85 model[3]. In fig. 3 the experimental data collected with the full MACRO length[16] are shown and compared to the predictions from extreme (proton dominated and iron dominated) composition models as taken from ref. [17]. Moreover, the overall agreement between simulation and data is maintained even when selecting restricted intervals of rock depth (probing different primary energies) and of zenith angle (probing different muon production height). This gives some confidence about the capability of the HEMAS code to describe the right correlation between $< P_t >$, $< E_\pi >$ and H (the meson production height).

On the basis of this code, MACRO has compared the experimental distribution of measured muon multiplicity to the prediction of two extreme composition models (the same used in the muon decoherence analysis), in order to establish its capability in separating different hypotheses about composition[18]. Prediction affirm that $< N_\mu >$ is sensitive to mass composition of the primary component (in practice to some power of $< A >$), since deep underground muons mainly come from the decay of mesons produced in the first stages of high energy interactions.

Practically independently from the composition model when selecting a muon multiplicity greater than 10, the primary energy/nucleus is at 90% c.l. beyond the knee region. In fig. 4 the comparison of experimental data with Monte Carlo predictions is shown. The analysis is relative to 3295 h of data taking ($\sim$ 150000 multiple muon events)[19]. In order to reproduce a statistical sample of the same order of that of experimental data, using HEMAS, a farm of 10 RISC machines has used about 2 months of total CPU time. Event generation requested 0.73 Gbytes of disk storage.

It may be of interest to notice how the treatment of muon transport at high energy is not a well assessed problem yet. There exist theoretical uncertainties on the nuclear screening in the muon bremsstrahlung cross section. This kind of systematics becomes numerically important at $E_\mu \geq 1\ TeV$. Most of present calculations concerning muon transport are based on the cross sections reviewed in ref. [20]; there the formulation of A.A.Petrukhin and V.V.Shestakov[21] for muon bremsstrahlung is adopted. Recently, in the framework of the design study for new hadron colliders, it has been pointed out[22] that the muon radiative energy loss in the TeV region as calculated from the formulas of ref. [20] are different from the results obtained with other formulations[23, 24]: discrepancies in the range 10÷20% were found. The problem can be traced in the nuclear screening terms adopted in ref. [21], as already pointed out in the review of ref. [24]. A recent confirmation of the necessity to change the nuclear screening factor comes from an experimental analysis of high energy cosmic muon energy loss in an iron-scintillator sampling calorimeter[25]. In that work the authors recalculate the cross section for muon bremsstrahlung, performing a numerical evaluation of the nuclear screening, using a standard two-component Fermi nuclear density. The use of the corrected screening brings to an increase in the probability of bremsstrahlung which is relevant in all calculations

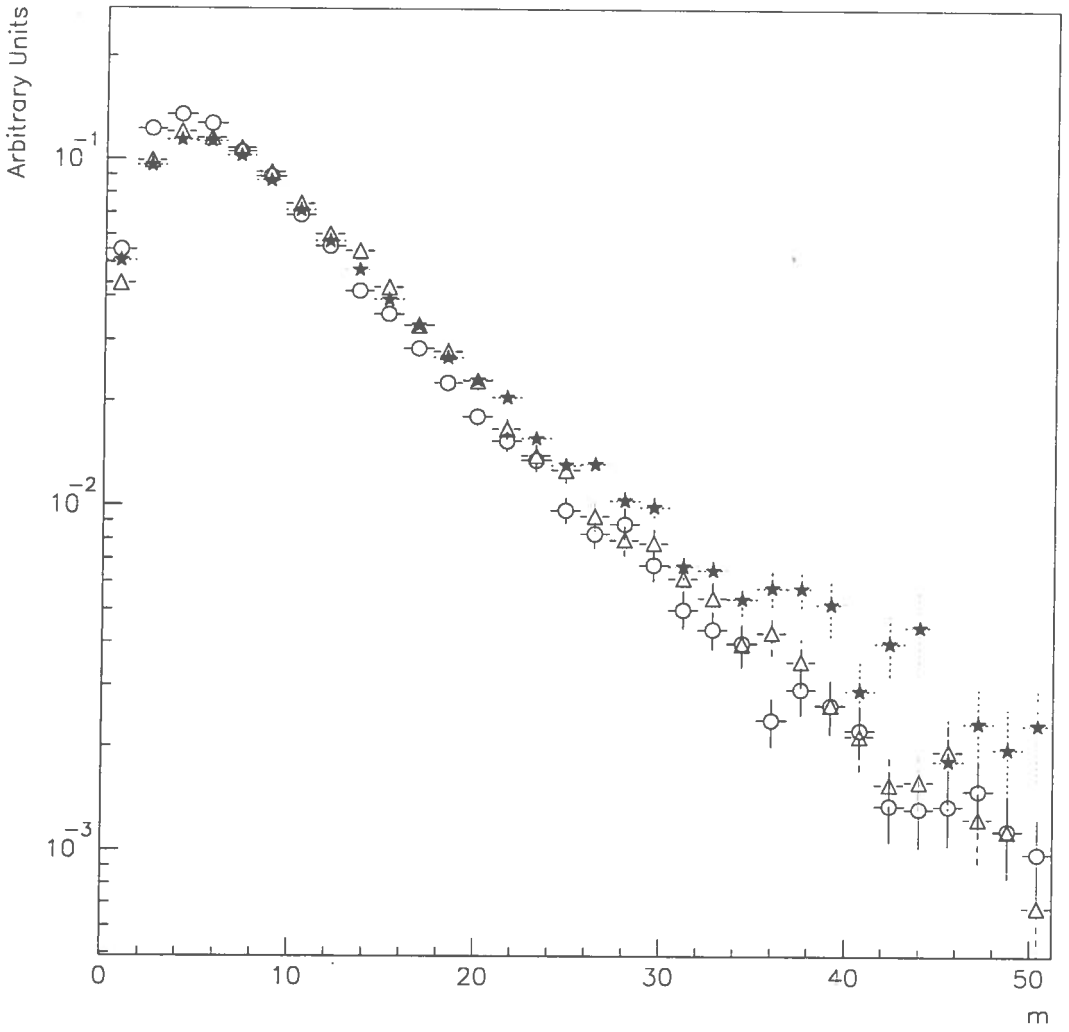

Figure 3. Separation distribution between muon pairs in MACRO. Black symbols are experimental data. The open symbols are the simulation with two extreme composition models (circles: light model, triangles: heavy model, see text)

11

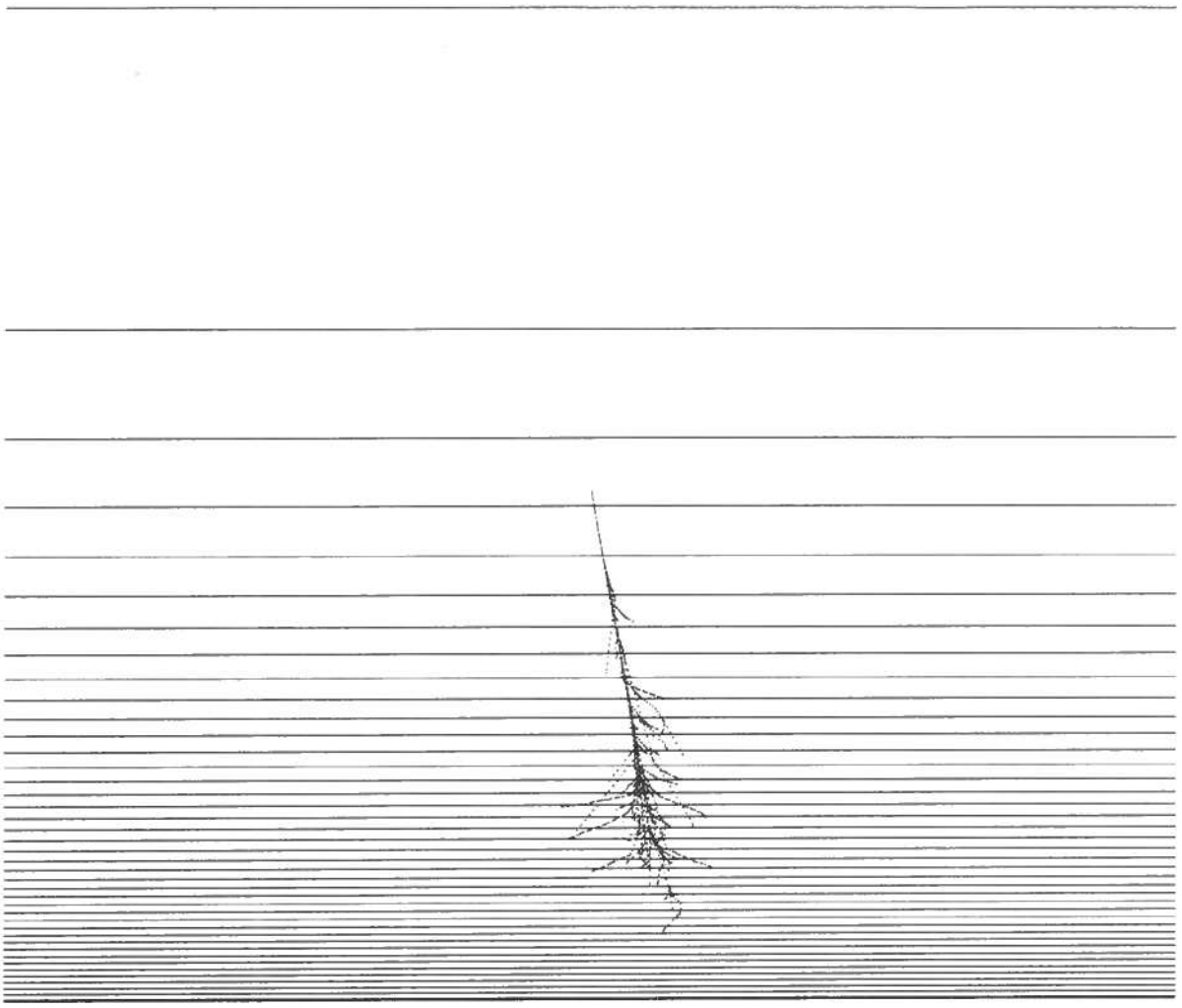

Figure 6. A 300 GeV electron shower in atmosphere, initiated at 60 gr/cm^2, as simulated using GEANT. (only secondaries with energy greater than 500 MeV are shown). The box structure reproducing the atmosphere, from 2 km to 36 km above sea level, is shown: each layer has a thickness of about 0.5 X_0. The horizontal scale is enlarged by a factor of 100 with respect to the vertical

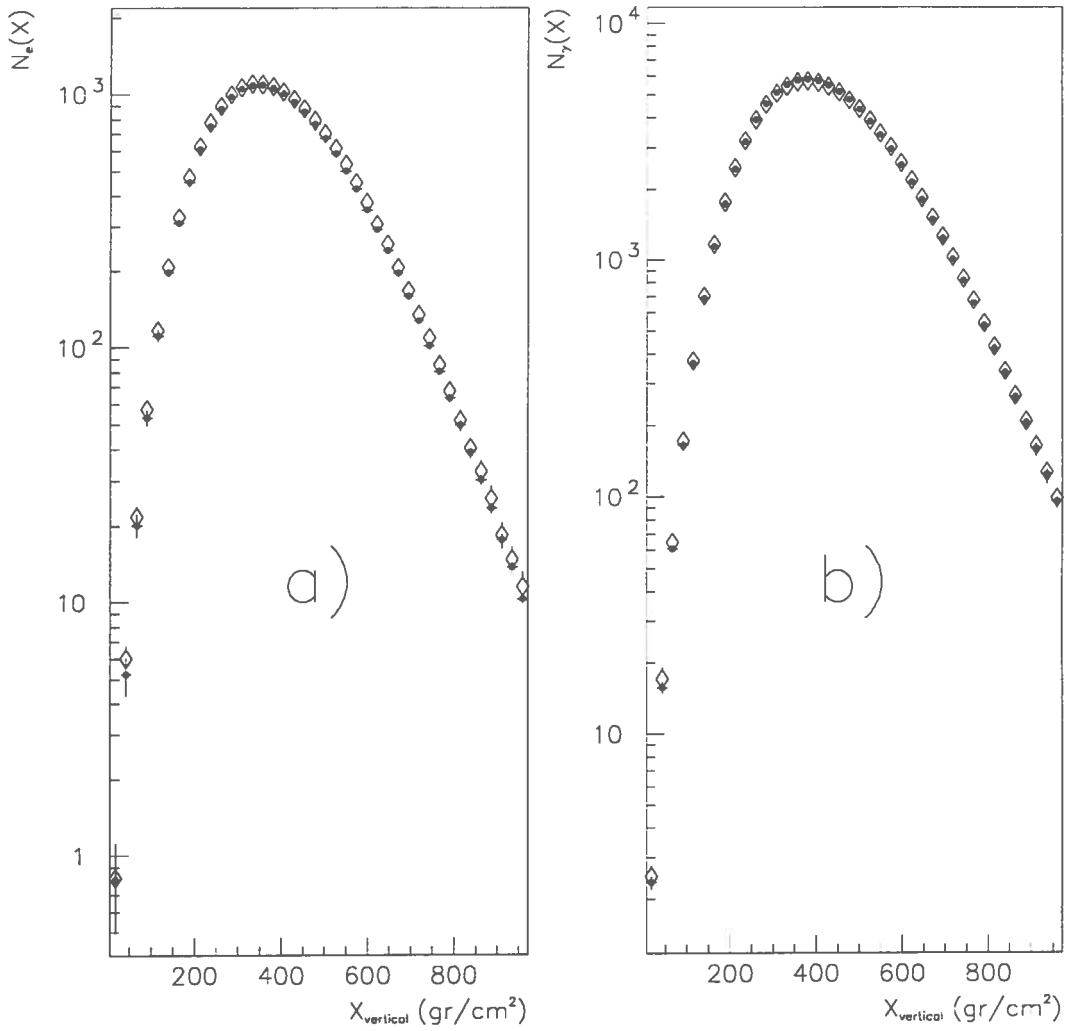

Figure 7. Longitudinal profiles of secondary electrons (a), and of secondary photons (b), for simulated 1 TeV gamma-initiated showers, as a function of atmospheric depth. Black symbols are the GEANT results, while the open ones are from FLUKA

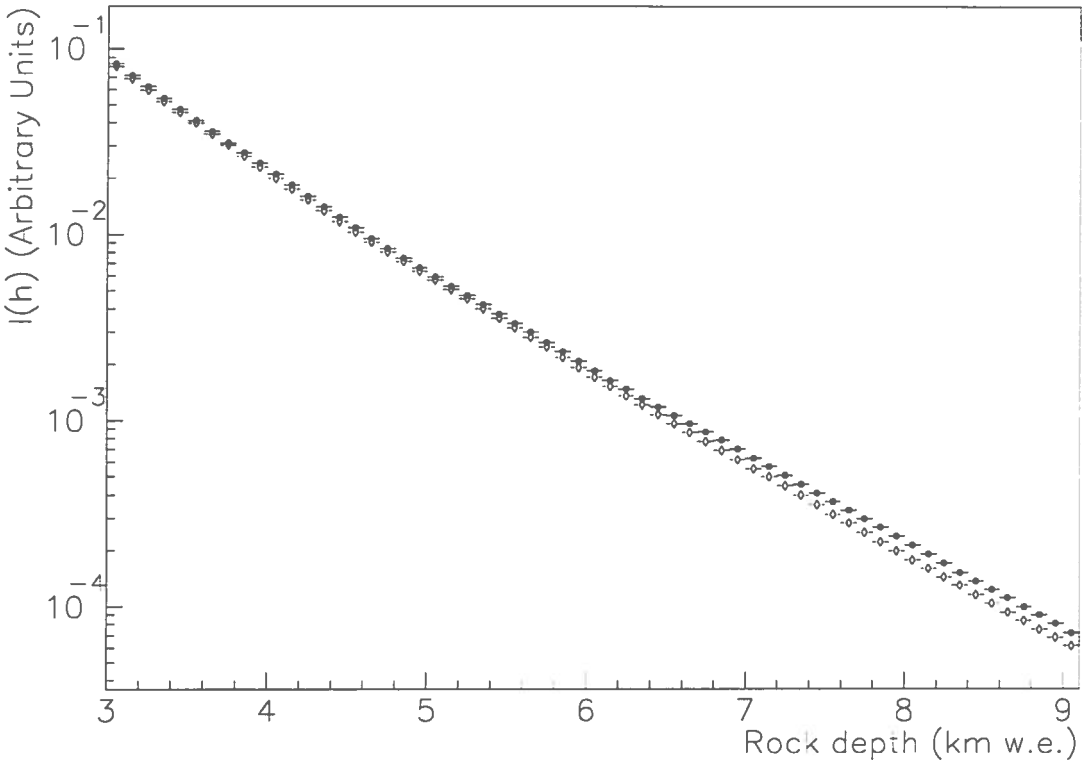

Figure 5. Muon intensity as a function of standard rock depth, assuming an atmospheric differential flux $\sim E^{-3.7}$. The lower points are the results with the new muon bremsstrahlung cross section

from X_{det} and X_{start}. GEANT version 3.15, and FLUKA have been adopted. For initial energy greater than 10 TeV only FLUKA has been used. The atmosphere is defined by a stack of box volumes of rectangular basis and thickness increasing with the height on the sea level. Any volume corresponds to a depth of 20 gr/cm^2. In each box the density is uniform and it is chosen in such a way that an approximation to the standard U.S. atmosphere is performed according to the quoted Shibata fit. The chosen depth granularity in our approximation is approximately one half of radiation length (37.66 gr/cm^2) in air. The exact relation between height and slant depth is the one shown in fig. 1 with the polygonal that represents the box approximation. The top of atmosphere has been limited at 5 gr/cm^2 (corresponding to a vertical height of $\simeq$ 36 Km), and the bottom is at 1025 gr/cm^2 (corresponding to the sea level). The same elementalcomposition has been used at all depths. The simulations have been performed on different platforms (HP-UX, IBM-AIX, VAX, and ALPHA DECStations). Particular care has been put in the choice of energy cut for secondary particles. It turns out that in practice a kinetic energy threshold of 1 MeV for all shower particles is enough. This is because real detectors are often shielded by an amount of material capable of absorbing most of low energy (less than 1 MeV) secondaries. The use of a lower energy cut results in a limited change on the energy flow at detector depth at the expense of a considerable amount of CPU. The possible consequences of the inclusion of geomagnetic field, approximated as a simple dipole has been tested: no appreciable effects were noticed.

An example of the simulation set-up is given in Fig. 6 which shows the development of a shower initiated by an electron of 300 GeV starting at a vertical atmospheric depth of 60 gr/cm^2; only secondary tracks with energy greater than 500 MeV are shown for clarity. In order to achieve a reliable parameterization of the relevant shower properties, sub-showers were generated at 17 different log-spaced energies, from 10 to 10^5 GeV, and at 16 different starting depth: from 10 to 760 gr/cm^2, in 50 gr/cm^2 steps.

It has been verified that at the boundary energies of $10^3 \div 10^4$ GeV the results of the GEANT and FLUKA, in air, are reasonably compatible. An example is shown in fig. 7. The existing differences are less from what can be expected by systematic effects, as for instance those arising by reasonable local variation of air pressure or composition with respect to the standard one.

The fundamental parameterizations are those of longitudinal profiles, radial, and energy distributions of the secondary particles. The knowledge of these functions allows to extract many necessary parameters for the analysis of surface array experiments. The longitudinal profile is sampled by counting the number of secondary particles crossing the boundary between the adjacent air regions in our simulation set-up. The number of secondary e^+e^- or photons, with energy greater or equal to a given cut, and for a given air thickness, can be extracted from the longitudinal profiles of the sub-showers. Such profiles can be easily fitted by a modified gamma function:

$$N_{e,\gamma}(t) = A \cdot t^{\alpha} \cdot e^{\beta \cdot t^{\gamma}} \tag{3}$$

The γ parameter can be omitted at all energies less or equal to 100 GeV, whitout loosing in the accuracy of the fit. It becomes necessary for higher energies. It is interesting to compare the results with the predictions from analytical solutions of shower equations. In Fig. 8 the longitudinal distribution of secondary e^+e^- and photons with energy exceeding 5 MeV as obtained in a gamma initiated sub-shower of energy of 1 TeV, starting at X_{start}= 10 gr/cm^2, is compared with the solution quoted in ref. [33]. It is clear how

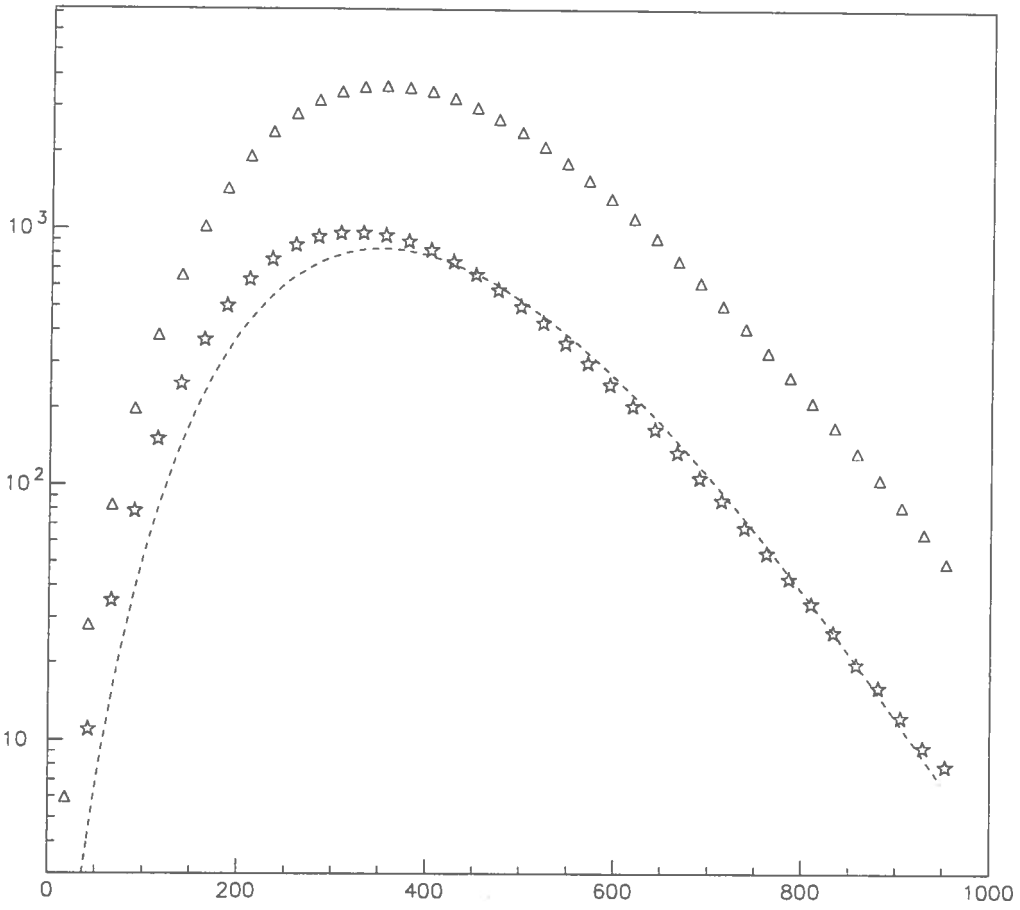

Figure 8. Longitudinal profiles of secondary electron (stars) and gammas (triangles) of energy $\geq 5MeV$ for a 1 TeV gamma shower initiated at 10 gr/cm^2. The dotted line is the analytical solution for secondary electrons quoted in the text. The horizontal scale is in gr/cm^2

the analytical formula accounts for the e^+e^- profile only in an approximate way, but the crucial point is that it completely ignores the contribution of secondary photons, which beyond the maximum exceeds that of electrons by a large factor. In a practical situation, if thick scintillator counters are used, a relevant number of these photons will interact in the sensitive medium, contributing significatively to the detected signal.

As expected the lateral distribution of secondary particles on a plane perpendicular to the shower axis is fitted, with reasonable approximation, by the Nishimura Kamata Greisen function[34]:

$$f(x) = \frac{\Gamma(4.5-s)}{2\pi\Gamma(s)\Gamma(4.5-2s)} x^{s-2}(1+x)^{s-4.5} \tag{4}$$

where $x = r/r_0$, r_0 being the Moliere radius; s is known as the age parameter, it has a unit value for a shower sampled at maximum development, and exceeds 1 if the shower is sampled after the maximum. An example of fit is shown in fig. 9, for secondary e^+e^- in a 1 TeV gammma initiated sub-shower, after a thickness of 460 gr/cm^2. At present also the calculation of the e.m. shower produced in atmosphere by hadrons of energy below 1 TeV is under progress, using the same kind of tools. A first application of the results here described have been used in the analysis[2] of the coincident detection of underground muons by MACRO and the e.m. component of EAS at 2000 m a.s.l. by the EAS-TOP experiment[35].

6. Conclusions and summary

The analysis of present cosmic ray experiments requires sophisticated simulation tools. The availability of powerful workstations has recently allowed a development of more detailed models, but it still remains a heavy task to collect a sample of simulated events statistically comparable with existing data. The possible application of parallel computing is still at experimental level.

The physics input is necessarily coming from accelerator data, however extrapolation to the very forward region is necessary. This operation seems to produce sensible results, but the systematic error introduced in the analysis by the existing models is still an open question.

The standard codes for shower simulation are finding application at a growing rate, at least to calibrate the specialised codes employed in this field.

7. Acknowledgements

I am indebted to the colleagues of the MACRO and EAS-TOP collaborations. In particular the following people provided invaluable help and material: C. Bloise, M. Carboni, C. Forti, P. Lipari, O. Palamara, V. Patera, S. Petrera, P. Vallania. Furthermore I wish to thank also T.K.Gaisser and T. Stanev, for useful discussions, and for providing software developments. A. Ferrari introduced me to the use of FLUKA, and to a deeper understanding of the underlying physics.

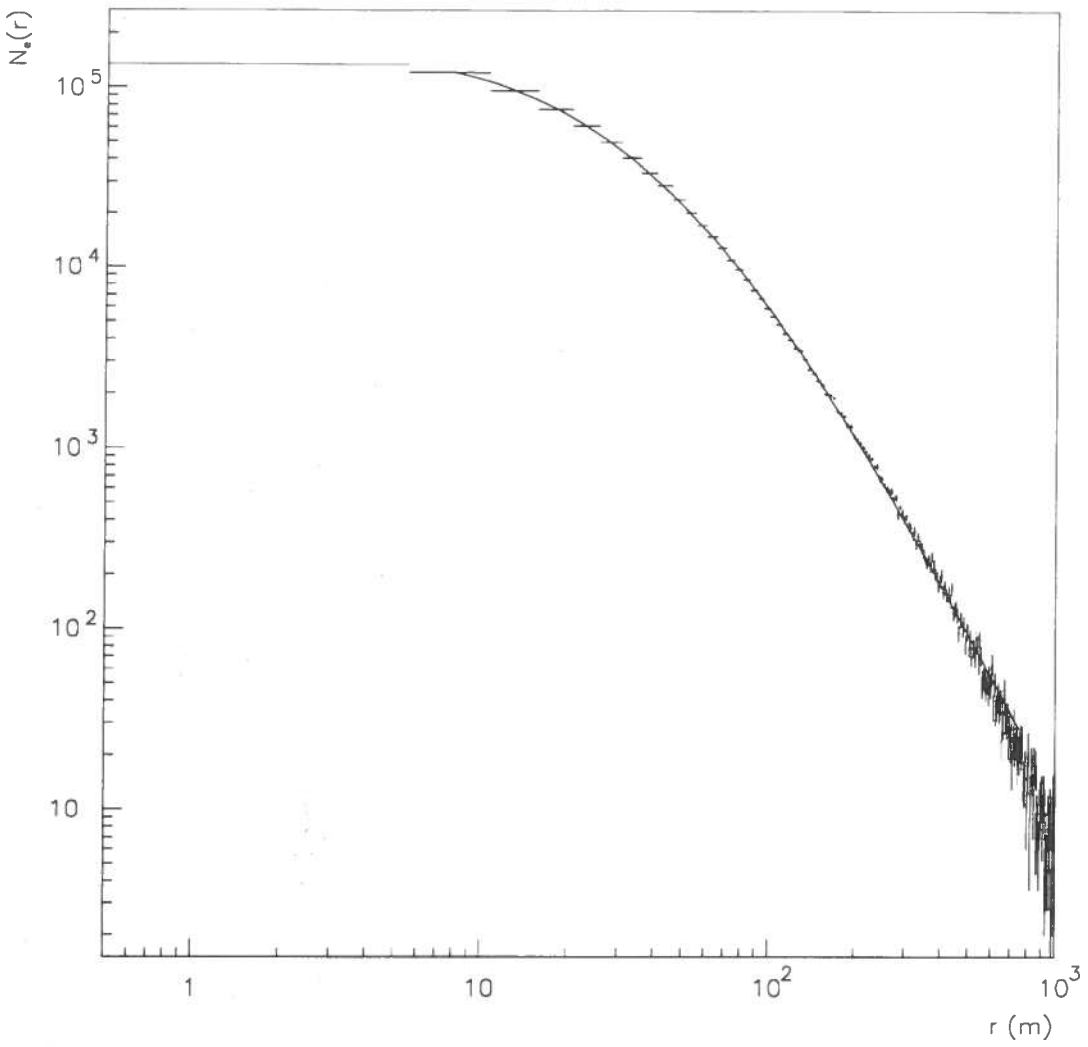

Figure 9. Radial distribution of secondary e^+e^- ($E \geq 1\ MeV$) for a 1 TeV gamma shower after 460 gr/cm^2. The fit to a NKG function is shown

REFERENCES

1. T.K. Gaisser, "Cosmic Rays and Particle Physics", Cambridge University Press, New York, 1990, and references therein.
2. MACRO and EAS-TOP Collaborations (R. Bellotti et al.), Phys. Rev. **D42** (1990) 1396. MACRO and EAS-TOP Collaborations, Proc. 23rd I.C.R.C., Calgary, **2** (1993) 89.
3. T.K Gaisser and T. Stanev, Nucl. Instr. & Meth. **A235** (1985) 183.
4. D.J. Bird et al., Proc. 23nd I.C.R.C., Calgary, **2** (1993) 34 and 38.
5. R.S. Fletcher et al., Proc. 23rd I.C.R.C., Calgary, **4** (1993) 40.
6. for a review see H.R. Schmidt and J. Schukraft, preprint GSI-92-19 (1992), published on Journ. of Modern Physics G.
7. A.M. Hillas, Proc. 17th I.C.R.C., Paris, **8** (1981) 193.
8. C. Forti et al., Phys. Rev. **D42** (1990) 3668.
9. G.J. Alner et al., Physics Letters **167B** (1986) 476.
10. P. Lipari et al, Proc. 22nd I.C.R.C., Dublin, **4** (1991) 197.
11. A. Capella and J. Tran Thang Van, A. Phys. **C10** (1981) 249.
12. T.K. Gaisser, Proc. Vulcano Workshop 1992 "Frontier Objects in Astrophysics and Particle Physics", **40** (1993) 433.
13. J. Engels et al., Proc. 22nd I.C.R.C., Dublin, **4** (1991) 1.
14. MACRO Collaboration (S.P. Ahlen et al.), Nucl. Instr. & Meth., **A324** (1993) 337.
15. MACRO Collaboration (S.P. Ahlen et al.), Phys. Rev. **D46** (1992) 4836.
16. MACRO collaboration, Proc. 23rd I.C.R.C., Calgary, **2** (1993) 93.
17. G. Auriemma et al., Proc. 21st I.C.R.C., Adelaide, **2** (1990) 101.
18. MACRO Collaboration (S.P. Ahlen et al.), Phys. Rev. **D46** (1992) 895.
19. MACRO collaboration, Proc. 23rd I.C.R.C., Calgary, **2** (1993) 97.
20. W. Lohmann, R. Kopp and R. Voss, CERN/85-03 (1985).
21. A.A. Petrukhin and V,V. Shestakov, Can. J. Phys **46** (1968) 5377.
22. M.J. Tannenbaum, CERN-PPE/91-134 (1991).
23. Y.S. Tsai, Rev. of Mod. Phys. **46** (1975) 815.
24. I.L.Rozental, Usp. Phys. nauk, **94** (1968) 91; Sov. Phys. Uspekhi **11** (1968) 49.
25. W.K.Sakumoto et al., Phys. Rev. **D45** (1992) 3042.
26. A. Fassó et al, "FLUKA92", presented at the Workshop on "Simulating Accelerator Radiation Environment", Santa Fé, January 1993, proceedings in press.
27. G. Battistoni and A. Ferrari, paper in preparation.
28. P. Lipari and T. Stanev, Proc. 23rd I.C.R.C., Calgary, **4** (1993) 411.
29. R. Brun et al., CERN GEANT 3 User's Guide, DD/EE/84-1 (1987).
30. W.R. Nelson, H. Hirayama and D.W.O. Rogers, report SLAC-265 (1985).
31. H.P. Vankov and T. Stanev, Proc. 23rd I.C.R.C., Calgary, **4** (1993) 167.
32. V. Patera, G. Battistoni, M. Carboni, A. Ferrari, P. Vallania, work in progress.
33. E. J. Fenyves et al., Phys. Rev **D37** no. 3 (1988) 649.
34. K. Greisen, "Progress in Cosmic Ray Physics", vol. 3 (1956)
35. EAS-TOP Collaboration (M. Aglietta et al.), Nucl. Instr. & Meth., **A277** (1989) 23.